

# In-band pumped erbium doped glass microspherical lasers

Snigdha Thekke Thalakkal<sup>a</sup>, Davor Ristić<sup>a</sup>, Stefano Pelli<sup>b</sup>, Daniele Farnesi<sup>b</sup>, Silvia Soria<sup>b</sup>, Hrvoje Gebavi<sup>a</sup>, Alessandro Chiasera<sup>c</sup>, Lidija Androš Dubraja<sup>a</sup>, Mile Ivanda<sup>a</sup>, Gualtiero Nunzi Conti<sup>b,\*</sup>

<sup>a</sup> Institute Ruđer Bošković, Bijenička Cesta 54, 10000, Zagreb, Croatia

<sup>b</sup> IFAC-CNR Istituto di Fisica Applicata “Nello Carrara”, Via Madonna del Piano 10, 50019, Sesto Fiorentino, FI, Italy

<sup>c</sup> IFN-CNR, CSMFO Lab. and FBK Photonics Unit, Via alla Cascata 56/C, 38123, Povo, TN, Italy

## ARTICLE INFO

Handling Editor: Dr P. Vincenzini

### Keywords:

Whispering gallery mode lasers  
Erbium doped glass  
Resonant pumping  
Thermal effects

## ABSTRACT

High-Q whispering gallery mode (WGM) microspherical resonators made in rare earth (RE) doped glasses are an ideal platform to implement compact and low threshold laser sources and represent a simple tool for the characterization of laser glasses and an ideal platform for several sensing applications. In the case of Erbium-doped glass, the conventional pumping is performed at 980 nm or at 1480 nm. In this work on erbium doped tellurite glass microspheres, we demonstrate WGM lasers with resonant pumping in the C telecom band using pump frequencies for which the absorption cross section is smaller than the emission cross section. Reduced thermal effects are observed, with laser emissions above 1600 nm.

## 1. Introduction

WGM microspherical lasers made in RE doped glasses have been studied extensively in the last decades since the first work of Sandoghdar et al. [1] on neodymium-doped silica glass, which followed the pioneering papers on  $\text{CaF}_2\text{:Sm}^{3+}$  crystals by Garrett et al. [2], and on dye doped ethanol droplets by Tzeng et al. [3]. A recent review on RE doped glass microlasers was published by Frigenti et al. [4], where the vast literature is summarized, including resonators with different shapes, RE dopants and glass matrices. These coherent, compact, and low threshold light sources, besides being a simple platform to test laser glasses – given their small size and ease of fabrication – came out to have their main applications in sensing [5] and biosensing [6]. Indeed, considering that the main sensing principle is based on monitoring the shift of the WGM resonance position, the strong narrowing (up to a few order of magnitude [7,8]) of the laser line compared to the cold cavity resonance linewidth translates into a corresponding significant improvement of the transducer sensitivity.

We recently proposed a simple fabrication method based on arc discharge to make microspheres in erbium doped tellurite glasses [9]. WGM microlasers in the wavelength region from 1.5  $\mu\text{m}$  to 1.61  $\mu\text{m}$  were then demonstrated by conventional pumping at 980 nm and at 1480 nm [9]. In this work we show that comparable results can be obtained by

resonant pumping in the C telecom band (1530 nm  $\div$  1565 nm), and particularly using pump wavelengths above 1550 nm, beyond those already exploited in similar glasses [10–12]. Importantly, high quality laser sources operating in this wavelength range are easily available and convenient. Compared to 980 nm pumping but also compared to 1480 nm, this approach allows improved mode and phase matching of the pump and signal WGMs, and strongly reduces heating effects. In fact, depending on the glass matrix and the related non-radiative transitions, conventional pumping of Erbium ions can strongly increase the microsphere temperature up to its melting point [9,13]. More generally, strong thermal effects can be detrimental for some applications like in case of biosensing when, for instance, DNA hybridization is performed on the resonator while it is lasing, and care has to be taken to avoid reaching temperature that can denature DNA [14].

## 2. Experimental

The experimental setup for the characterization of the Erbium-doped microspheres is shown in Fig. 1. A fiber pigtailed tunable laser (semiconductor external cavity laser NetTest TUNICS-Plus CL) operating in the C and L band (1530 nm  $\div$  1625 nm) is used as pump source as well as to measure the cold cavity WGM quality factor. A polarization controller allows selecting the input polarization state while an attenuator is used

\* Corresponding author.

E-mail address: [g.nunziconti@ifac.cnr.it](mailto:g.nunziconti@ifac.cnr.it) (G. Nunzi Conti).

<https://doi.org/10.1016/j.ceramint.2024.12.036>

Received 15 October 2024; Received in revised form 29 November 2024; Accepted 2 December 2024

Available online 2 December 2024

0272-8842/© 2024 The Author(s). Published by Elsevier Ltd. This is an open access article under the CC BY license (<http://creativecommons.org/licenses/by/4.0/>).

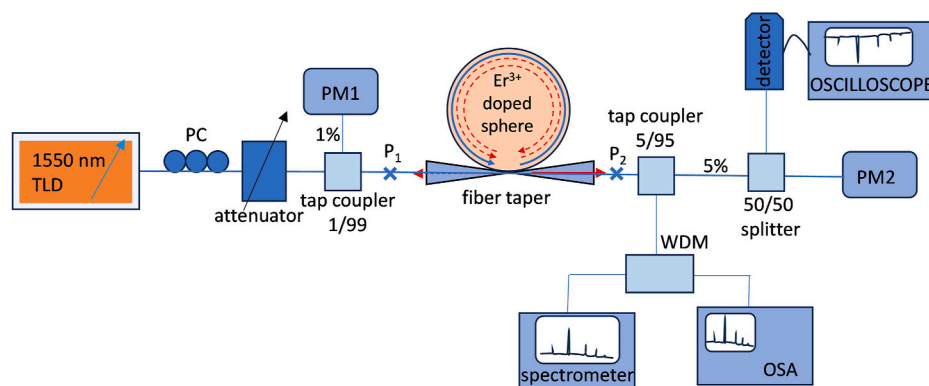


**Fig. 1.** Experimental setup for the characterization of the microsphere lasers. TLD: tunable laser diode; PC: polarization controller; PM: power meter; WDM: wavelength division multiplexer; OSA: optical spectrum analyzer.

to change the pump power without affecting the laser wavelength. In fact, if the pump power is increased by raising the current, we observe a wavelength shift up to 8 pm/mW (when operating in the sweeping mode) even if the wavelength value set in the benchtop mainframe is kept fixed. The input power  $P_i$  is monitored using a 1/99 power splitter by sending the 1 % output to a power meter. The light is evanescently coupled to the resonator using a home-made fiber taper of about 3  $\mu\text{m}$  fabricated in a standard SMF-28 fiber and with typical transmission losses of about 1.5 dB. The same taper is also used to collect the laser signal and the photoluminescence from the microsphere. A 1550 nm fused tap coupler (optical ratio 95/5) at the output section is followed on the low power branch by a 50/50 splitter. One output of the splitter is sent to a power meter to measure the 1550 nm residual pump power while the other output is sent to a photodiode to monitor the presence of a resonance when the pump laser is used in the scanning mode. When a high Q resonance is observed it is then possible to thermally lock the pump to the same resonance [15] and the scanning mode can be terminated to proceed with the measurements. The 95 % branch of the tap coupler is sent to a 1550 nm fused fiber power splitter that acts as wavelength division multiplexer (WDM) for the fundamental modes [16] to separate the photoluminescence and lasing in the C and L band – which are sent to an Optical Spectrum Analyzer (AQ6317B from Ando, 600 nm–1750 nm range) – from the upconversion emissions (at wavelength below 1000 nm [10,17]), which are sent to a CCD spectrometer (SPM-002-XT64 from Photon Control).

### 3. Results and discussion

The zinc-tellurite glass (75TeO<sub>2</sub>-20ZnO-5Na<sub>2</sub>O, mol%) doped with 1 mol % of Erbium was fabricated by melting batches composed of analytical grade of the constituents with a process similar to that described in Ref. [18]. In a previous paper we have shown that of the three concentrations we used (0.5 %, 1 %, 2 %), the 1 % concentration produces the best results [19].

Differential scanning calorimetry was performed on zinc-tellurite glass and on zinc-tellurite glass doped with 1 mol% Erbium to determine the thermal properties and glass stability. DSC signal was measured during heating and cooling cycles in the temperature range from 293 to 773 K in an extra pure nitrogen environment at a rate of 10 K min<sup>-1</sup>. Erbium doping has a significant influence on the increase of the glass transition temperature ( $T_g = 583$  K compared to 574 K for undoped glass) and the crystallization temperature ( $T_c = 758$  K compared to 725 K for undoped glass) of 75TeO<sub>2</sub>-20ZnO-5Na<sub>2</sub>O glasses. In addition, the doped glass shows better stability against devitrification with  $T_c - T_g = 175$  K.

After crushing the glass in powder of submillimeter grains, the microspheres were then synthesized using the plasma torch method described in Ref. [9], obtaining diameter sizes in the range between 11

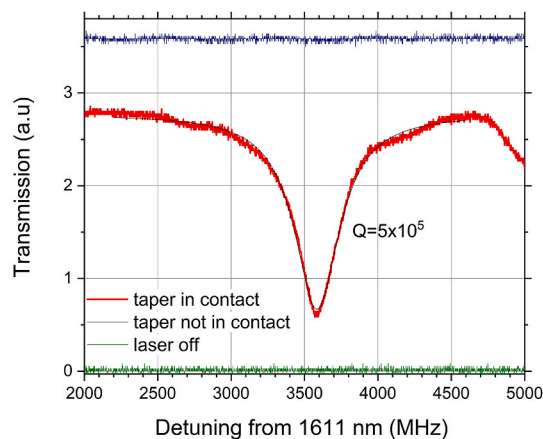


**Fig. 2.** WGM resonance of an Erbium-doped tellurite glass microsphere of 41  $\mu\text{m}$  in diameter showing a loaded Q factor of  $5 \times 10^5$  (red curve). The measurement was performed around 1611 nm, i.e. outside the absorption band of Erbium. The blue line is the taper transmission before being placed in contact with the microsphere. (For interpretation of the references to colour in this figure legend, the reader is referred to the Web version of this article.)

$\mu\text{m}$  and 88  $\mu\text{m}$ . Using this method, larger spheres came out somewhat irregularly shaped and therefore they were not suitable for WGM lasing. A tapered fiber tip covered with glue was then used to pick up the

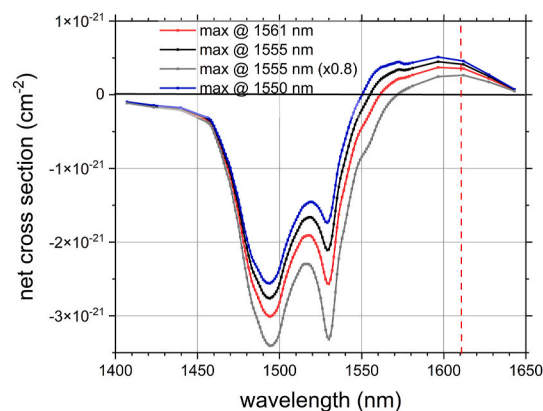


**Fig. 3.** Maximum net cross section of Erbium-doped tellurite glass calculated for different pumping wavelengths. The grey line assumes 80 % of the maximum inversion level when pumping at 1555 nm. (For interpretation of the references to colour in this figure legend, the reader is referred to the Web version of this article.)

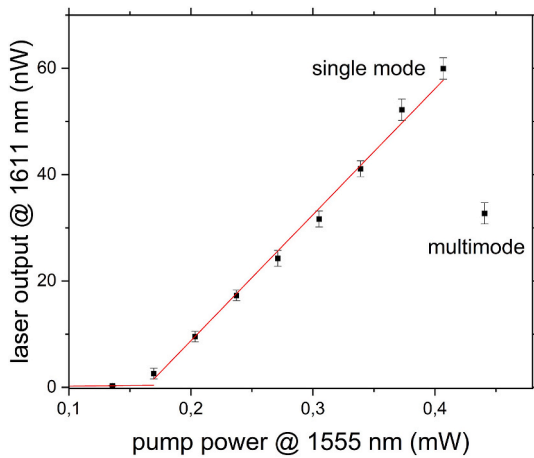


**Fig. 4.** Characteristic curve of an Erbium-doped tellurite glass microsphere (42  $\mu\text{m}$  in diameter) showing the taper coupled output power vs the absorbed pump power. The laser is single mode up to about 400  $\mu\text{W}$  of absorbed pump power and then it becomes multimode.

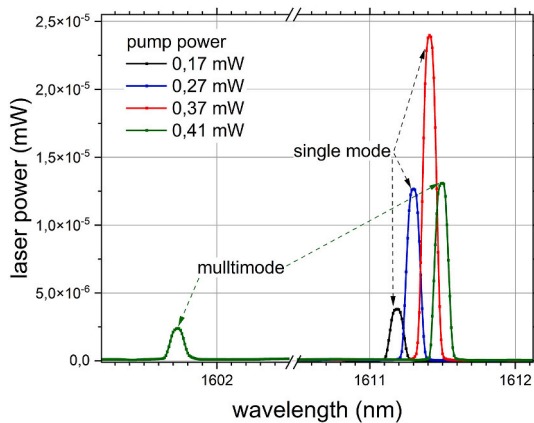


**Fig. 5.** Laser spectra from the same microsphere of Fig. 4 collected between 1601 nm and 1612 nm with an OSA (0.1 nm wavelength resolution) at the output of the coupling fiber taper for different pump power values at 1555 nm (For interpretation of the references to colour in this figure legend, the reader is referred to the Web version of this article.)

spheres one by one for easy handling and characterization. Spheres smaller than 20  $\mu\text{m}$  were not used because they were too difficult to glue.

The refractive index of the glass is 1.996 at 1550 nm [18]. Because of the big difference in refractive index of the silica fiber, higher order WGM were coupled [20]. Moreover, part of the light was radiated out of the fiber when the taper got in contact with the microsphere, as shown in Fig. 2. The same figure also shows a typical resonance measured around 1611 nm (outside the absorption band of the Erbium ions), with a loaded Q factor of  $5 \times 10^5$ . The microsphere diameter is 41  $\mu\text{m}$ .

The pump laser could be easily thermally locked to a similar resonance within the C band and wavelength in the range between 1550 nm and 1561 nm were considered. In this wavelength range absorption cross section is smaller than emission cross section [18]. The maximum in band pumping inversion rate  $N_{\text{max}}$  between the  $^4I_{15/2}$  level and the  $^4I_{13/2}$  level of Erbium ions corresponds to the transparency condition at the pump wavelength  $\lambda_p$ , i.e.  $N_{\text{max}} = \sigma_a(\lambda_p)/(\sigma_a(\lambda_p) + \sigma_e(\lambda_p))$ , where  $\sigma_a(\lambda_p)$  and  $\sigma_e(\lambda_p)$  are the absorption and emission cross sections, respectively [21]. For glass with similar composition as the one used in our experiment [18]  $N_{\text{max}} = 0.38$  when pumping at 1550 and  $N_{\text{max}} = 0.33$  when pumping at 1561 nm, and the corresponding maximum net cross sections are shown in Fig. 3. The wavelength range with the highest positive

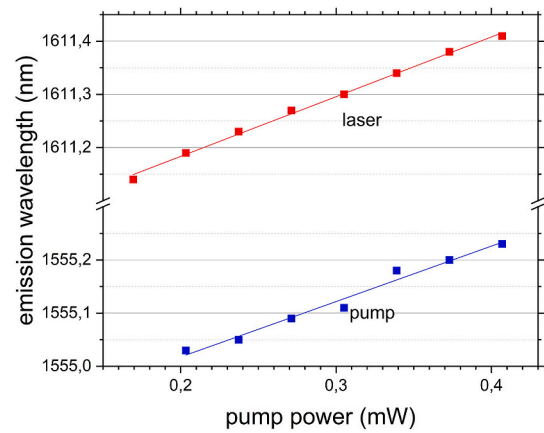


**Fig. 6.** Laser wavelength shift with increasing pump power (red line). Optimal pump wavelength can be adjusted for maximum laser emission, resulting in an almost identical shift (blue line,  $\sim 1 \text{ pm}/\mu\text{W}$ ). The microsphere is the same as Fig. 4. (For interpretation of the references to colour in this figure legend, the reader is referred to the Web version of this article.)

cross section is around 1600 nm but if maximum inversion rate is not reached then it further shifts toward larger wavelengths as shown in Fig. 3 for 1555 nm pumping (for 80 % of the maximum inversion rate). Indeed, it was in the band between 1600 nm 1611 that lasing could be consistently obtained both in single mode and multimode regimes.

The characteristic curve for a microsphere laser with a diameter of 42  $\mu\text{m}$  is shown in Fig. 4. The pump wavelength is 1555 nm and the single mode emission is around 1611 nm. Pump power refers to the power coupled to the microsphere or more correctly to the difference between the pump power at the taper output before and after contact with the microsphere. This latter is sometimes called ‘absorbed’ power, but it also includes power radiated outside the sphere (and not coupled to it, as shown in Fig. 2). In this case, when the pump is locked to the resonance, the absorbed power is about one third of the launched one and the threshold for laser emission is about 160  $\mu\text{W}$  for the curve in Fig. 4. During the measurements the taper is kept in contact with the microsphere to improve the system stability. Laser output power refers to the laser signal collected by the taper in the forward direction. The error bars are standard deviation from measurements performed every 15 s for 5 min after each pump power increase. The emission is single mode up to a pump power of 400  $\mu\text{W}$  when it becomes multimode as shown in the laser spectra of Fig. 5 taken for increasing pump power. As expected, the single mode laser wavelength slightly shifts because of thermal effects and the consequent temperature increase of the microsphere. As shown in Fig. 6, a red shift is observed, consistently with the values of the thermal expansion coefficient ( $\alpha_R = 1/R \cdot dR/dT \sim -11.5 \times 10^{-6} \text{ K}^{-1}$ ) and the thermo-optic coefficient ( $dn/dT \sim 16.2 \times 10^{-6} \text{ K}^{-1}$ ) around room temperature of tellurite glasses having the same composition [22], and according to the formula  $d\lambda_r/dT = \lambda_r(\alpha_R + 1/n \cdot dn/dT)$ , where  $\lambda_r$  is the resonance wavelength,  $R$  is the sphere radius, and  $n$  is the refractive index [23]. From the calculated value of the resonance wavelength shift with temperature ( $d\lambda_r/dT = 12 \text{ pm/K}$ ) and the measured overall shift of the laser wavelength (270 pm for pump power increasing from 0.17 mW to 0.41 mW, corresponding to 1.1  $\text{pm}/\mu\text{W}$ ), we can assume a corresponding temperature increase of the microsphere of 22 K when the pump increases from the laser threshold to the multimode behavior (0.24 mW of pump power increase). A similar shift (1  $\text{pm}/\mu\text{W}$ ), also shown in Fig. 6, is obtained if slightly adjusting the thermally locked pump wavelength for maximizing the laser output.

Monitoring the thermal effects from the laser wavelength shift allows assessing the temperature increase in the microsphere. In RE-doped glasses a well-known method to sense temperature is based on the fluorescence intensity ratio (FIR) technique [24,25], which, in the case of Erbium ions implies measuring the intensity ratio of the two

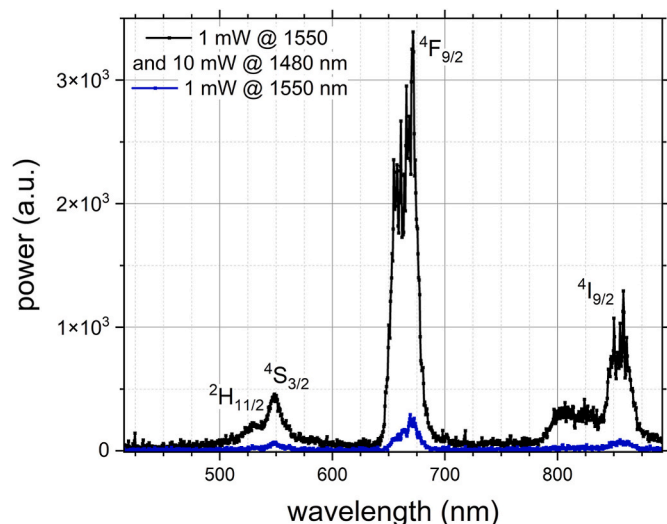


**Fig. 7.** Upconversion luminescence spectra of Erbium ions from several energy levels to the ground state  $^4I_{15/2}$  in the range 400 nm–900 nm. Light is collected by evanescent coupling to the fiber taper from the same microsphere of Fig. 4. To clearly resolve the green upconversion levels the limited power of the 1550 nm laser (1 mW) was not enough (blue line) and an additional pump at 1480 nm was used (black line). (For interpretation of the references to colour in this figure legend, the reader is referred to the Web version of this article.)

upconversion green emission lines centered at 525 nm and 550 nm [26, 27]. However, in our system, when pumping above 1550 nm and with rather low power (below 0.5 mW, as shown in Fig. 4), the detected green upconversion was too weak to reliably perform FIR measurement, as shown in Fig. 7. In fact, in the green upconversion process, three pump photons at 1550 nm are involved to reach the  $^2H_{11/2}$  and  $^4S_{3/2}$  levels. Moreover, as expected, the very poor efficiency of the evanescent coupling from the microsphere WGMs to the taper modes at visible wavelengths (the evanescent field decay constant in the radial direction goes with the inverse of the wavelength [28,29]), strongly reduces the collected signal in that portion of the spectrum. In order to more clearly identify the contributions to upconversion luminescence of the various energy levels we also used an additional pump at 1480 nm and the results are presented in Fig. 7. Green luminescence could be collected with or without lasing around 1600 nm, but there was no evidence of a green upconversion laser as in Refs. [10,17,30].

#### 4. Conclusions

WGM lasers emitting above 1600 nm in Erbium-doped tellurite glass microspheres with diameters around 40  $\mu\text{m}$  were demonstrated by in band resonant pumping in the region 1550 nm  $\div$  1560 nm. Thermal effects due to nonradiative decays are strongly reduced compared to pumping at 980 nm and 1480 where similar glasses can rise their temperature up to their transition value  $T_g$ . By monitoring the single mode laser wavelength shift we showed that our system had a temperature increase limited to 20 K. Such a limited temperature rise would allow, for instance, the implementation of ultra-high resolution WGM DNA-based biosensors operating at temperatures well below DNA denaturation.

#### CRediT authorship contribution statement

**Snigdha Thekke Thalakkal:** Investigation. **Davor Ristić:** Conceptualization. **Stefano Pelli:** Writing – review & editing. **Daniele Farnesi:** Writing – review & editing. **Silvia Soria:** Writing – review & editing. **Hrvoje Gebavi:** Investigation. **Alessandro Chiasera:** Writing – review & editing. **Lidija Androš Dubraja:** Investigation. **Mile Ivanda:**

Conceptualization. **Gualtiero Nunzi Conti:** Conceptualization.

#### Data availability statement

The data that supports the findings of this study are available upon request from the corresponding author.

#### Funding

Croatian Science Foundation IP-2019-04-3045; Croatian Government and the European Union through the European Regional and Development Fund - the Competitiveness and Cohesion Operational Programme (KK.01.1.1.01.0001).

#### Declaration of competing interest

The authors declare that they have no competing financial interests or personal relationships that could have appeared to influence the work reported in this paper.

#### Acknowledgements

Mr. Franco Cosi from IFAC-CNR is gratefully acknowledged for fabricating fiber tapers.

#### References

- [1] V. Sandoghdar, F. Treussart, J. Hare, V. Lefèvre-Seguin, J.-M. Raimond, S. Haroche, Very low threshold whispering-gallery-mode microsphere laser, *Phys. Rev. A* 54 (1996) R1777–R1780, <https://doi.org/10.1103/PhysRevA.54.R1777>.
- [2] C.G.B. Garrett, W. Kaiser, W.L. Bond, Stimulated emission into optical whispering modes of spheres, *Phys. Rev.* 124 (1961) 1807–1809, <https://doi.org/10.1103/PhysRev.124.1807>.
- [3] H.-M. Tzeng, K.F. Wall, M.B. Long, R.K. Chang, Laser emission from individual droplets at wavelengths corresponding to morphology-dependent resonances, *Opt. Lett.* 9 (1984) 499–501, <https://doi.org/10.1364/OL.9.000499>.
- [4] G. Frigenti, S. Berneschi, D. Farnesi, S. Pelli, G.C. Righini, S. Soria, Y. Dumeige, P. Féron, D. Ristić, F. Prudenzi, M. Ferrari, G. Nunzi Conti, Rare earth-doped glass whispering gallery mode micro-lasers, *Eur. Phys. J. Plus.* 138 (2023) 679, <https://doi.org/10.1140/epjp/s13360-023-04275-9>.
- [5] T. Reynolds, N. Riesen, A. Meldrum, X. Fan, J.M.M. Hall, T.M. Monro, A. François, Fluorescent and lasing whispering gallery mode microresonators for sensing applications, *Laser Photon. Rev.* 11 (2017) 1600265, <https://doi.org/10.1002/lpor.201600265>.
- [6] N. Toropov, G. Cabello, M.P. Serrano, R.R. Gutha, M. Rafti, F. Vollmer, Review of biosensing with whispering-gallery mode lasers, *Light Sci. Appl.* 10 (2021) 42, <https://doi.org/10.1038/s41377-021-00471-3>.
- [7] A. François, M. Himmelhaus, Whispering gallery mode biosensor operated in the stimulated emission regime, *Appl. Phys. Lett.* 94 (2009) 031101, <https://doi.org/10.1063/1.3059573>.
- [8] J. Yang, L.J. Guo, Optical sensors based on active microcavities, *IEEE J. Sel. Top. Quant. Electron.* 12 (2006) 143–147, <https://doi.org/10.1109/JSTQE.2005.862953>.
- [9] S. Thekke Thalakkal, D. Ristić, G. Nunzi Conti, S. Pelli, G. Frigenti, H. Gebavi, A. Chiasera, M. Ivanda, Er<sup>3+</sup>-doped tellurite whispering gallery mode microlasers in 1.5  $\mu\text{m}$ –1.61  $\mu\text{m}$  wavelength region generated by 0.98  $\mu\text{m}$  and 1.48  $\mu\text{m}$  pump lasers, *Opt. Mater.* X 19 (2023) 100248, <https://doi.org/10.1016/j.omx.2023.100248>.
- [10] X. Wang, Y. Yu, S. Wang, J.M. Ward, S.N. Chormaic, P. Wang, Single mode green lasing and multicolor luminescent emission from an Er<sup>3+</sup>-Yb<sup>3+</sup> co-doped compound fluorosilicate glass microsphere resonator, *OSA Contin.* 1 (2018) 261–273, <https://doi.org/10.1364/OSAC.1.000261>.
- [11] E.A. Anashkina, A.V. Andrianov, Erbium-doped tellurite glass microlaser in C-band and L-band, *J. Lightwave Technol.* 39 (2021) 3568–3574, <https://doi.org/10.1109/JLT.2021.3064999>.
- [12] A.V. Andrianov, E.A. Anashkina, Thermo-optical control of L-band lasing in Er-doped tellurite glass microsphere with blue laser diode, *Opt. Lett.* 47 (2022) 2182–2185, <https://doi.org/10.1364/OL.455468>.
- [13] J.M. Ward, P. Feron, S. Nic Chormaic, A taper-fused microspherical laser source, *IEEE Photon. Technol. Lett.* 20 (2008) 392–394, <https://doi.org/10.1109/LPT.2008.916904>.
- [14] A. Blanco, G. Blanco, Chapter 6 - nucleic acids, in: A. e Blanco, G. Blanco (Eds.), *Medical Biochemistry Second Edition*, Academic Press, 2022, pp. 131–152, a c. di.
- [15] T. Carmon, L. Yang, K.J. Vahala, Dynamical thermal behavior and thermal self-stability of microcavities, *Opt. Express* 12 (2004) 4742–4750, <https://doi.org/10.1364/OPEX.12.004742>.
- [16] D. Garcia-Rodriguez, M. Morant, J.L. Corral, R. Llorente, Modal selectivity at 850 nm employing standard single-mode couplers: theory and experimental

- demonstration, *Opt Commun.* 436 (2019) 248–252, <https://doi.org/10.1016/j.optcom.2018.12.003>.
- [17] B. Jiang, Y. Hu, L. Ren, H. Zhou, L. Shi, X. Zhang, Four- and five-photon upconversion lasing from rare earth elements under continuous-wave pump and room temperature, *Nanophotonics* 11 (2022) 4315–4322, <https://doi.org/10.1515/nanoph-2022-0360>.
- [18] G.N. Conti, V.K. Tikhomirov, M. Bettinelli, S. Berneschi, M. Brenici, B. Chen, S. Pelli, A. Speghini, A.B. Seddon, G.C. Righini, Characterization of ion-exchanged waveguides in tungsten tellurite and zinc tellurite Er<sup>3+</sup>-doped glasses, *Opt. Eng.* 42 (2003) 2805–2811, <https://doi.org/10.1117/1.1604782>.
- [19] S.T. Thalakkal, D. Ristić, G.N. Conti, S. Pelli, G. Frigenti, H. Gebavi, A. Chiasera, M. Ivanda, Plasma torch produced Er<sup>3+</sup>-doped tellurite whispering gallery mode microresonator for lasing application, in: *Novel Optical Systems, Methods, and Applications XXVI*, SPIE, 2023 1266502.
- [20] A. Chiasera, Y. Dumeige, P. Féron, M. Ferrari, Y. Jestin, G. Nunzi Conti, S. Pelli, S. Soria, G.c. Righini, Spherical whispering-gallery-mode microresonators, *Laser Photon. Rev.* 4 (2010) 457–482, <https://doi.org/10.1002/lpor.200910016>.
- [21] E.-L. Lim, S. Alam, D.J. Richardson, High-energy, in-band pumped erbium doped fiber amplifiers, *Opt Express* 20 (2012) 18803–18818, <https://doi.org/10.1364/OE.20.018803>.
- [22] A. Koike, N. Sugimoto, 1. Temperature dependences of optical path length in inorganic glasses, *Rep. Res. Lab. Asahi Glass Co Ltd.* 56 (2006).
- [23] M. Brenici, R. Calzolari, F. Cosi, G.N. Conti, S. Pelli, G.C. Righini, Microspherical resonators for biophotonic sensors, in: *Lightmetry and Light and Optics in Biomedicine*, SPIE, 2004, pp. 225–233, 2006.
- [24] P. Haro-González, I.R. Martín, L.L. Martín, S.F. León-Luis, C. Pérez-Rodríguez, V. Lavín, Characterization of Er<sup>3+</sup> and Nd<sup>3+</sup> doped Strontium Barium Niobate glass ceramic as temperature sensors, *Opt. Mater.* 33 (2011) 742–745, <https://doi.org/10.1016/j.optmat.2010.11.026>.
- [25] H. Berthou, C.K. Jörgensen, Optical-fiber temperature sensor based on upconversion-excited fluorescence, *Opt. Lett.* 15 (1990) 1100–1102, <https://doi.org/10.1364/OL.15.001100>.
- [26] D. Manzani, J.F. da S. Petrucci, K. Nigoghossian, A.A. Cardoso, S.J.L. Ribeiro, A portable luminescent thermometer based on green up-conversion emission of Er<sup>3+</sup>/Yb<sup>3+</sup> co-doped tellurite glass, *Sci. Rep.* 7 (2017) 41596, <https://doi.org/10.1038/srep41596>.
- [27] Z. Cai, A. Chardon, H. Xu, P. Féron, G. Michel Stéphane, Laser characteristics at 1535 nm and thermal effects of an Er:Yb phosphate glass microchip pumped by Ti: sapphire laser, *Opt Commun.* 203 (2002) 301–313, [https://doi.org/10.1016/S0030-4018\(02\)01114-8](https://doi.org/10.1016/S0030-4018(02)01114-8).
- [28] Y. Panitchob, G.S. Murugan, M.N. Zervas, P. Horak, S. Berneschi, S. Pelli, G. N. Conti, J.S. Wilkinson, Whispering gallery mode spectra of channel waveguide coupled microspheres, *Opt Express* 16 (2008) 11066–11076, <https://doi.org/10.1364/OE.16.011066>.
- [29] A. Chiasera, Y. Dumeige, P. Féron, M. Ferrari, Y. Jestin, G. Nunzi Conti, S. Pelli, S. Soria, G.c. Righini, Spherical whispering-gallery-mode microresonators, *Laser Photon. Rev.* 4 (2010) 457–482, <https://doi.org/10.1002/lpor.200910016>.
- [30] T. Lu, L. Yang, R.V.A. van Loon, A. Polman, K.J. Vahala, On-chip green silica upconversion microlaser, *Opt. Lett.* 34 (2009) 482–484, <https://doi.org/10.1364/OL.34.000482>.